Qualitative change in structural dynamics of some glass-forming systems

V. N. Novikov and A. P. Sokolov

Phys. Rev. E **92**, 062304 — Published 14 December 2015

DOI: 10.1103/PhysRevE.92.062304

Qualitative change in structural dynamics of some glass-forming systems

V.N. Novikov[1], A.P. Sokolov[1,2]

[1]*Department of Chemistry and Joint Institute for Neutron Sciences, University of Tennessee, Knoxville, TN 37996, USA*

[2]*Chemical Sciences Division, Oak Ridge National Laboratory, Oak Ridge, TN 37831, USA*

Abstract

Analysis of temperature dependence of structural relaxation time $\tau(T)$ in supercooled liquids revealed a qualitatively distinct feature - a sharp, cusp-like maximum in the second derivative of $\log \tau_\alpha(T)$ at some T_{max}. It suggests that the super-Arrhenius temperature dependence of $\tau_\alpha(T)$ in glass-forming liquids eventually crosses over to an Arrhenius behavior at $T<T_{max}$, and there is no divergence of $\tau_\alpha(T)$ at non-zero T. T_{max} can be above or below T_g, depending on sensitivity of $\tau(T)$ to change in liquid's density quantified by the exponent γ in the scaling $\tau_\alpha(T) \sim \exp(A/T\rho^{-\gamma})$. These results might turn the discussion of the glass transition to the new avenue – the origin of the limiting activation energy for structural relaxation at low T.

1. Introduction

The structural relaxation in glass-forming liquids usually shows Arrhenius-like behavior at high temperatures, $\tau_\alpha(T) = \tau_0 \exp(E_\infty/T)$, but becomes super- Arrhenius at lower temperatures [1,2]. Moreover, the steepness of the temperature dependence of $\log(\tau_\alpha)$ vs $1/T$ increases sharply with cooling (Fig.1a), meaning that the activation energy for structural relaxation, $E(T)$, increases with decreasing T. This suggests that the relaxation time and activation energy might diverge at some finite, non-zero temperature, indicating existence of an underlying phase transition at $T < T_g$ [2]. Attempts to resolve this fundamental question of $\tau_\alpha(T)$ divergence from detailed analysis of experimental data thus far provided different conclusions [3-6]. The authors of [3] found no evidence for the divergence of the structural relaxation time. In ref. [4] it was shown that the divergent signature of τ_α disappears below T_g in amber. On the other hand, detailed analysis of the relaxation time in poly(vinyl acetate) revealed the VFT-like behavior of τ_α extends far below T_g (at least by 4 orders) [5,6].

To describe $\tau_\alpha(T)$ various functions were proposed. The most common are three parameter functions: Vogel-Fulcher-Tammann (VFT) function

$$\tau_\alpha = \tau_0 \exp(B/(T-T_{VFT}) \text{ [7-9]}; \quad (1)$$

double-Arrhenius [10]

$$\tau_\alpha = \tau_0 \exp[(B/T)\exp(E/T)], \quad (2)$$

Bässler-Avramov's [11,12]

$$\tau_\alpha = \tau_0 \exp(C/T^\alpha) \quad (3)$$

and parabolic [13]

$$\tau_\alpha = \tau_0 \exp[(J/T_0)^2 (T_0/T\text{-}1)^2] \qquad (4)$$

functions. They are based on various phenomenological models, e.g. free-volume [14] and configurational entropy [15], elastic [16], Random First Order Transition (RFOT) [17] and facilitation [18] models, etc. These models either predict the underlying phase transition with diverging relaxation time at finite T (e.g. free volume, entropy based Adam-Gibbs and RFOT), or predict no divergence of $\tau_\alpha(T)$ for any T except at $T = 0$ K. These functions fit the temperature variations of structural relaxation time reasonably well. In some materials they provide good description in the entire temperature range above T_g, e.g., VFT function fits τ_α(T) in polymers or glycerol very well at all T. However, they give different predictions on the divergence of τ_α(T). This divergence would correspond to the divergence of the size of the cooperatively rearranging regions in the Adam-Gibbs approach [15] or of the correlation radius in the Random First Order Theory [17]. Even if there is no divergence of the relaxation time at non-zero T, still there is a question does activation energy $E(T)$ diverges as temperature goes to zero (as suggested by e.g. double-Arrhenius equation (2))?

To have deeper understanding of the temperature dependence of $\tau_\alpha(T)$ and to discriminate between various models one should look on more subtle features of the $\tau_\alpha(T)$ behavior. Recent developments in experimental techniques, especially in broadband dielectric spectroscopy, provide highly accurate experimental data that can reveal these subtle changes in $\tau_\alpha(T)$. Here we present new analysis of the temperature dependence of viscosity or τ_α of supercooled liquids based on their second derivative. We show that at least in some supercooled liquids there is a qualitatively distinct feature in the second derivative of $\tau_\alpha(T)$ that resembles a cusp-like singularity with a sharp maximum. This maximum is not predicted by any of the discussed above 3-parameter functions. Presented analysis suggests that the equilibrium $\tau_\alpha(T)$ turns to Arrhenius-

like behavior also at low temperatures, so there is no divergence of $\tau_\alpha(T)$ or $E(T)$ at a finite temperature. The activation energy, in contrast, approach some constant value apparently related to the limited activation energy required for structural relaxation.

2. Derivative Analysis

As a first example, we consider the classical glass forming liquid salicylic acid (salol) [19]. The structural relaxation time of salol can be fit reasonably well by several functions discussed above (Fig.1a). The first derivative of $\log\tau_\alpha$ over T_g/T presents the apparent activation energy that increases monotonically with temperature decrease (Fig. 1b). However, the second derivative of the experimental data reveals a sharp peak at a temperature $T_{max} = 255$ K (Fig.2a). A few other independent data for $\tau_\alpha(T)$ of salol [20-22] also reproduce this cusp-like peak in the second derivative. For example, the second derivative of the structural relaxation time of salol measured by a different group [20] (Fig. 2a) exhibits the same peak at the same T_{max} (with accuracy better than 1K). Similar behavior can be found in some other glass-forming systems where the sufficiently accurate data on the relaxation time or viscosity are available [23, 24, 25]. For example, the second derivative of $\log\tau_\alpha(T)$ exhibits the sharp maximum in phenylphthalein dimethyl ether (PDE) and polychlorinated biphenyl with chlorine content 62% (PCB62) (Fig.3); and the second derivative of the $\log\eta$ for the covalent-bonding B_2O_3 [25] also exhibits maximum at $T_{max} \sim 630$K (Fig. 4).

However, there are not so many data with accuracy required for the second derivative analysis. The dimensionless second derivative of $\log_{10}\tau$ or $\log_{10}\eta$ over T_g/T has the amplitude about a few hundred, up to 600 (Figs. 2-6). Experimental data on the relaxation time have errors that are

reflected in some scattering of the data points of $\tau(T)$. Taking derivatives greatly increases the scattering. A simple estimation can be done based on about 20-30 experimental data points in the interval $0.5 < T_g/T < 1$. The typical interval between the data points $\Delta(T_g/T)$ in this case is about 0.02- 0.03 that will enhance the error of $\log\tau$, $\Delta\log\tau$, in the second derivative by a factor of about $\sim 10^3$. If one wants the resulting error to be, e.g., only 10% of the actual value of the second derivative, then the error $\Delta\log_{10}\tau \approx (\log_{10}e)\Delta\tau/\tau \approx 0.43\Delta\tau/\tau$ should be less than a few percent. The analysis of large amount of published data revealed that the scattering of the second derivative points in most cases is too high to provide any conclusive results.

Analysis of a broad number of glass forming liquids with sufficiently accurate data revealed some systems that do not exhibit the peak in the second derivative of $\log\tau$ in supercooled state. They include hydrogen-bonding liquids, polymers and room-temperature ionic liquids (RTIL). As examples, we show the second derivative of $\log_{10}\tau_\alpha$ in glycerol and propylene carbonate (PC) (Fig.5), and in tri-cresylphosphat (m-TKP), ethanol, polyvinylacetate (PVAc) and [bmim][NTf2] (Fig.6).

3. Discussion

We note, that the second derivative of $\log\tau_\alpha$ over T_g/T is proportional to the first derivative of the apparent activation energy

$$E_a = d\ln\tau_\alpha/d(1/T) \qquad (5)$$

The maximum in the second derivative means that the rate with which E_a is growing upon cooling drastically changes behavior at T_{max}: The rate increases with decreasing temperature at $T > T_{max}$, while it sharply decreases with further cooling below T_{max}. In logarithmic scale, the peak in the second derivative of $\log\tau_\alpha$ can be described by two linear regimes with positive and negative slopes and intersection at $T = T_{max}$ (Figs.2-4). It means that $\log_{10}[(\log_{10}\tau_\alpha)''] = a +$

$b(T_g/T)$ where a and b are some constants, $b > 0$ at $T > T_{max}$ and $b < 0$ at $T < T_{max}$. This corresponds to Arrhenius behavior of $(\log_{10}\tau_\alpha)''$ with the activation energy changing sign at T_{max}:

$$(\log_{10}\tau_\alpha)'' = A_1\exp(E_1/T) \text{ at } T>T_{max} \qquad (6a)$$

$$(\log_{10}\tau_\alpha)'' = A_2\exp(-E_2/T) \text{ at } T<T_{max}. \qquad (6b)$$

For salol, $A_1=7.8*10^{-3}$, $A_2=3.91*10^3$, $E_1 = 2803$K, $E_2 = 2337$K. The apparent activation energy E_a , Eq. (5), can be obtained by integrating $(\log_{10}\tau_\alpha)''$:

$$E_a = B_1 + \frac{A_1 T_g^2 \ln 10}{E_1}\exp\left(\frac{E_1}{T}\right), \qquad T > T_{max} \qquad (7a)$$

$$E_a = E_0 - \frac{A_2 T_g^2 \ln 10}{E_2}\exp\left(-\frac{E_2}{T}\right), \qquad T < T_{max} \qquad (7b)$$

where B_1 and E_0 are constants, $B_1 = E_\infty - A_1 T_g^2 \ln 10/E_1 \approx E_\infty$. Eqs.(7a), (7b) predict that there are two Arrhenius regimes: One at high temperatures (with $E_a = E_\infty$ which is well documented [30]), and another one at low temperature ($E_a = E_0$). The activation energy rises with cooling at intermediate temperatures and then saturates at some level. A characteristic temperature interval for the decaying exponential in Eq. (7b) is $\Delta T \sim T_g*(T_g/E_2) \sim 20$K for salol, i.e. the respective interval is $\Delta(T_g/T) \sim 0.1$. At such distance from T_{max}, behavior of $\tau_\alpha(T)$ becomes close to the Arrhenius again. We note that this low-temperature Arrhenius behavior is related to the equilibrium supercooled liquid and is different from the Arrhenius behavior below T_g observed in non-equilibrium glass-formers. Similarly, the slowdown of the rate of increase of τ_α at lowering temperature below T_{max} (Fig.1b) occurs at temperatures where τ_α is still short enough ($\sim 10^{-4}$ s) and the liquid is in equilibrium, so a systematic error that leads to such behavior is unlikely.

It is important to emphasize that the maximum in the second derivative challenges all the discussed above traditional 3-parameter fitting functions. They produce a monotonic second

derivative without any peak (some examples are shown in Fig.3). Thus they all failed to reproduce accurately the temperature variations of $(\log\tau_\alpha)''$ in these liquids even qualitatively in this temperature range. However, there is a four-parameter function derived by Cohen and Grest (CG) [31] in the free-volume percolation model of the glass transition that has the maximum in the second derivative of $\log\tau_\alpha$:

$$\log_{10}(\tau_\alpha/\tau_0) = \frac{2B}{T-T_0+\sqrt{(T-T_0)^2+aT}} \quad . \tag{8}$$

Here T_0 may be both higher and lower than T_g, depending on material. The parameter a is determined by the anharmonicity of the intermolecular potential. It is known that the CG function fits very well the experimental data for $\tau_\alpha(T)$ and $\eta(T)$ in various glass-formers at all T [31,32] . This is not surprising because the CG function has an additional parameter in comparison with the VFT function. The latter is the limiting case of the CG function at $a \to 0$. The second derivative of the CG function over inverse temperature indeed has a maximum at

$$T_{max} = \frac{T_0}{1-\frac{a}{2T_0}} \quad , \tag{9}$$

although it is not as sharp as the experimental one (Figs. 2-4). Thus, the position of the peak of the second derivative can be determined by simple fitting experimental $\tau_\alpha(T)$ or $\eta(T)$ to the CG function (Eq.(8)). Since the ratio a/T_0 is small, ~0.01÷0.1 (Refs. [31,32]), for practical purposes T_0 gives a good estimate of T_{max} with accuracy of a few percent.

As it was mentioned in Section 2, some supercooled liquids do not show the peak in the second derivative of $\tau_\alpha(T)$ (Figs.5,6). Fit to the CG function (Eq. (8)) gives T_0 ~160K for glycerol which is below its T_g (Fig.5a). This may explain why there is no peak in the second derivative of $\log\tau_\alpha$ in the supercooled glycerol and some other glass-formers: the peak is expected to be at

temperatures below T_g, where the equilibrium supercooled state cannot be reached experimentally. As one of the consequences, a single VFT or other 3-parameter functions mentioned above can fit $\tau_\alpha(T)$ of glycerol and other materials with T_0 below T_g reasonably well in the entire temperature range of supercooled state. This explains the well-known fact that $\tau_\alpha(T)$ in polymers [33], RTIL [29] and some hydrogen-bonding materials [26] can be fit well by a single VFT function, while many molecular liquids require at least two VFT functions, one for low temperatures and another one for high temperatures [19]. We emphasize that the proposed here existence of the maximum in the second derivative of τ_α at T_{max} ($\sim T_0$) below T_g is a speculation based on the fit to the CG function and is not confirmed experimentally. The only justification of this point is that in all cases, when the CG fit provides $T_0 > T_g$ and the data are good enough to analyze the second derivative, there is the maximum at $T_{max} \sim T_0$. It would be important to perform an experiment when a parameter of a glass-former or external conditions, such as pressure, can be varied in order to change the ratio T_0/T_g from $T_0/T_g<1$ to $T_0/T_g > 1$ and track the evolution of the respective peak of the second derivative of $\log\tau_\alpha$. We note that the CG fit in the case of propylene carbonate estimates $T_0 \sim T_g$ (Fig.5). Although the peak is not resolved (Fig. 5b), the data are consistent with a possible peak at $T \sim T_g$.

The critical question is what controls the position of T_{max} ($\sim T_0$) with respect to T_g? The exact physical meaning of the temperature T_{max} is not clear, but in the CG model $T_{max} \sim T_0 = T_1 + a/4 \sim T_1$, where T_1 is a parameter showing the sensitivity of the anharmonic part of the inter-particle potential to changing volume [31]. Thus, the stronger anharmonicity of the potential depends on volume, the higher will be T_{max} with respect to some reference material temperature, such as melting or glass transition temperature. Thus, the ratio T_{max}/T_g might correlate with the sensitivity of the structural relaxation time to changing volume. The dependence of the

structural relaxation in glass-forming liquids on volume V can be characterized by the exponent γ of the so-called thermodynamic scaling [34,35]:

$$\tau(T) = \tau_0 \exp(A/TV^{\gamma}) \qquad (10)$$

The larger is γ the stronger is the dependence of τ_α on volume. Analysis of γ and T_0 obtained using CG fit revealed that the ratio T_0/T_g indeed increases with increasing γ (Fig. 7). These data suggest that $T_0 > T_g$ in glass-formers with $\gamma \geq 3.5 \div 4$, which are mostly molecular liquids. The peak of the second derivative can be experimentally detected only in such liquids. Materials with $\gamma < 3.5$ (hydrogen-bonding materials, many polymers, RTILs) have $T_0 \leq T_g$. In these materials the peak is predicted to be at temperatures where the supercooled liquid falls out of equilibrium, and thus the peak cannot be observed experimentally.

The presented analysis suggests the following scenario: (i) Glass-forming liquids exhibit Arrhenius-like temperature dependence of the structural relaxation time (viscosity) at high temperatures; (ii) at intermediate temperatures the apparent activation energy for structural relaxation $E_a(T)$ increases upon cooling, and $\tau_\alpha(T)$ exhibits super-Arrhenius behavior; (iii) this increase, however, slows down upon further cooling and (iv) eventually $E_a(T)$ reaches a limiting value, leading to a low-temperature Arrhenius behavior of $\tau_\alpha(T)$ with a constant activation energy E_0. Unfortunately, the low-temperature Arrhenius regime in pure form is not observable due to rather long relaxation time required (see e.g. Fig.1b for salol). We want to stress here that this low-temperature Arrhenius is expected in equilibrium supercooled liquid. It should not be confused with the non-equilibrium Arrhenius behavior usually observed at $T < T_g$.

In the Adam-Gibbs [15] and RFOT [17] theories, the activation energy is proportional to the volume of the cooperatively rearranging region (CRR). The crossover to the low-temperature

Arrhenius regime means that the size of CRR does not diverge with cooling, and instead, after initial growth eventually saturates at some maximum value. Recently, the low-temperature Arrhenius regime was predicted in a string model [36]. In this model CRR corresponds to strings comprised of fast moving molecules. Applying the theory of living polymers to the strings, the authors showed that the string length increases upon cooling, but will saturate at some limited length at lower temperatures. This would correspond to the limited size of CRR, and consequently, of the activation energy. In elastic models [16] the low-temperature Arrhenius behavior corresponds to the limiting value of shear modulus. In any case, regardless the microscopic mechanism, the activation energy E cannot grow to infinitely large value and will have its limit that depends on the material. Indeed, there should be a limiting energy cost for a molecule to make a relaxation motion in a supercooled liquid. Thus relaxation in any glass-forming liquid eventually will become Arrhenius-like upon cooling and no divergence of time scale at finite T should be expected.

According to Fig. 2, the third order derivative, i.e., the slope of $(\log\tau_\alpha)''$, has a finite jump at T_{max} in salol, and, respectively, the fourth order derivative is infinite at T_{max}. In the Adams-Gibbs thermodynamic theory of glass transition $\log\tau_\alpha/\tau_0 = \text{const}/TS_c(T)$ [15] where $S_c(T)$ is the configurational entropy. Thus, $S_c(T)$ should have infinite fourth order derivative at T_{max}. This formally means that the system experiences a subtle fourth order phase transition at T_{max}. At this point we do not have a clear physical picture of the nature of this transition. We speculate that at decreasing temperature the collective relaxation eventually acquires such high activation energy and CRR size that at $T < T_{max}$ either CRR size is limited by the mechanism of relaxation, as in the string model [36], or another channels of relaxation with limited collectivity have equal or higher rate.

We note that the peak in B_2O_3 (Fig.4) looks different from all other cases – it is strongly asymmetric. It is known that B_2O_3 exhibits a structural transformation above T_g, with increasing number of B_3O_6 boroxol rings at the expense of BO_3 triangular units [37]. We cannot exclude that the observed maximum in $(\log_{10}\eta)''$ in B_2O_3 (Fig. 4) is related to this structural change. However, observation of the maximum in the second derivative of several other liquids (Fig.2, 3), and a correlation of T_0/T_g with the scaling parameter γ point to a more general nature of the transition.

The temperature T_{max} at which the increase in $E(T)$ starts to slow down, differs with respect to T_g for different materials and it may be lower or higher than T_g depending on sensitivity of structural relaxation to change in volume (density) (Fig.7). Thus there are systems where crossover to the low-temperature Arrhenius behavior is visible (e.g. salol, PDE, PCB65, B_2O_3), but there are systems where this should happen only at $T < T_g$. This explains why attempts to analyze divergence of $\tau_\alpha(T)$ at finite T in various systems [3-6] may produce different results: There are systems (apparently with high γ) where no divergence can be obvious at $T \sim T_g$, while this regime cannot be achieved in other systems, where $T_{max} < T_g$.

4. Conclusions

In conclusion, the second derivative of the temperature dependence of the structural relaxation time and viscosity in some supercooled liquids exhibits a sharp maximum. Such a maximum is not predicted by traditional three-parameter functions suggested for description of $\tau_\alpha(T)$. Thus, these functions are missing important qualitative feature of the glass transition. This behavior of the second derivative suggests that the super-Arrhenius dependence of $\tau_\alpha(T)$ should eventually cross over to an Arrhenius regime at further cooling and there is a limiting value for the activation energy required for structural relaxation. The crossover to this low-temperature

Arrhenius regime can be both above and below T_g, apparently depending on the sensitivity of the structural relaxation of the material to change in volume. This provides a hint to parameters that might define the maximum activation energy for structural relaxation of the liquid. Employing this approach might help to reveal many other peculiarities of dynamics in Soft Matter.

Acknowledgments: We acknowledge the support from the NSF Chemistry program (grant CHE-1213444). We are grateful to P. Griffin for useful discussions and bringing our attention to the Cohen-Grest function and to M. Roland for providing experimental data for segmental relaxation in PMMA with different molecular weights.

References

[1] P.G. Debenedetti & F.H. Stillinger, Nature **410**, 259 (2001).

[2] S.A. Kivelson and G. Tarjus, Nature Mat. **7**, 831 (2008).

[3] T. Hecksher, A.I. Nielsen, N.B. Olsen, & J.C. Dyre, Nature Phys. **4**, 737 (2008).

[4] J. Zhao, S.L. Simon, and G.B. McKenna, Nature Commun. **4**, 1783 (2013).

[5] R. Richert, Physica A **287**, 26 (2000).

[6] R. Richert, J. Phys. Chem. **139**, 137101 (2013).

[7] H. Vogel, Phys. Zeit. **22**, 645 (1921).

[8] G.S. Fulcher, J. Am. Ceram. Soc. **8**, 339 (1925).

[9] G. Tammann, J. Soc. Glass Technol. **9**, 166 (1925).

[10] J.C. Mauro, Y. Yue, A.J. Ellison, P.K. Gupta, and D.C. Allan, Proc. Nat. Ac. Sci. **46**, 19780 (2009).

[11] H. Bässler, Phys. Rev. Lett. **58**, 767 (1987).

[12] I. Avramov, A. Milchev, J. Non-Cryst. Solids **104**, 253 (1988).

[13] Y. Elmatad, J.P. Garrahan, D. Chandler, J. Phys. Chem. B **113**, 5563 (2009).

[14] M.H. Cohen, and D. Turnbull, J. Chem. Phys. **31**, 1164 (1959).

[15] G. Adam, & J.H. Gibbs, J. Chem. Phys. **43**, 139 (1965).

[16] J.C. Dyre, Rev. Mod. Phys. **78**, 953 (2006).

[17] V. Lubchenko and P.G. Wolynes, Ann. Rev. Phys. Chem. **58**, 235 (2007).

[18] D. Chandler, and J.P. Garrahan, Annu. Rev. Phys. Chem. **61**, 191 (2010).

[19] F. Stickel, E.W. Fischer, and R. Richert, J. Phys. Chem. **102**, 6251 (1995).

[20] B. Schmidtke, N. Petzold, R. Kahlau, M. Hofmann, and E. A. Rössler, Phys. Rev. E 86, 041507 (2012)

[21] Y. Yang and K.A. Nelson, Phys. Rev. Lett. **74**, 4883 (1995).

[22] L. Wu, P.K. Dixon, S.R. Nagel, B.D. Williams, and J.P. Carini, Journal of Non-Crystal. Sol. **131-133**, 32 (1991).

[23] F. Stickel, E.W. Fischer, and R. Richert, J. Phys. Chem. **102**, 2043 (1996).

[24] M. Paluch, R. Casalini, and C.M. Roland, Phys. Rev. E **67**, 021508 (2003).

[25] A. Napolitano, P.B. Macedo, and E.G. Hawkins, J.Am.Cer.Soc. **48**, 613 (1965).

[26] N. Menon, K.P. O'Brien, P.K. Dixon, L. Wu, S.R. Nagel, B.D. Williams, and J.P. Carini, J. Non-Cryst. Sol. **141**, 61 (1992).

[27] F.-J. Stickel, *Untersuchung der Dynamik in niedermolekularen Flüssigkeiten mit Dielektrischer Spektroskopie. PhD Thesis, Universität Mainz* (Shaker, Aachen, 1995).

[28] C.M. Roland, Macromolecules **43**, 7875 (2010).

[29] P.G. Griffin, A.L. Agapov, A.P. Sokolov, Phys. Rev. E **86**, 021508 (2012).

[30] V.A. Popova, and N.V. Surovtsev, Phys. Rev. E **90**, 032308 (2014).

[31] M.H. Cohen, and G.S. Grest, Phys. Rev. B **20**, 1077 (1979).

[32] S. Corezzi, S. Capaccioli, R. Casalini, D. Fioretto, M. Paluch, P.A. Rolla, Chem. Phys. Lett. **320**, 113 (2000).

[33] J.D. Ferry, *Viscoelastic properties of polymers* (Wiley, New York, 1980).

[34] C. Alba-Simionseco, A. Cailliaux, A. Alegria, and G. Tarjus, Europhys. Lett. **68**, 58 (2004).

[35] R. Casalini, and C.M. Roland, Phys. Rev. B **71**, 014210 (2004).

[36] B. A. P. Betancourt, J. F. Douglas, and F. W. Starr, J. Chem. Phys. 140, 204509 (2014).

[37] A. C. Wright, G. Dalba, F. Rocca, N.M. Vedishcheva, Phys. Chem. Glasses: Eur. J. Glass Sci. Technol. B **51**, 233 (2010); M. Misawa, J.Non-Cryst. Sol.**122**, 33 (1990).

[38] A. Döß, M. Paluch, H. Sillescu, and G. Hinze, Phys. Rev. Lett. **88**, 095701 (2002).

[39] C.M. Roland, S. Hensel-Bielowka, M. Paluch, and R. Casalini, Rep. Prog. Phys. **68**, 1405 (2005).

[40] N. Menon, K.P. O'Brien, P.K. Dixon, L. Wu, S.R. Nagel, B.D.Williams, and J.P. Carini, J. Non-Cryst. Sol. **141**, 61 (1992).

[41] P. Sillren, et al. J. Chem. Phys. **140**, 124501 (2014).

[42] E.R. López, A.S. Pensado, M.J.P. Comuñas, A.A.H. Pádua, J. Fernández, and K.R. Harris, J. Chem. Phys. **134**, 144507 (2011).

[43] P. Lunkenheimer, R. Wehn, U. Schneider, and A. Loidl, Phys. Rev. Lett. **95**, 055702 (2005).

[44] G. Floudas, M. Paluch, A. Grzybowski, K.L. Ngai, *Molecular dynamics of glass-forming systems* (Springer, New York, 2011).

[45] S. Hensel-Bielówka, M. Paluch, and K.L. Ngai, J. Chem. Phys. **123**, 014502 (2005).

[46] A. Reiser, G. Kasper, S. Hunklinger, Phys. Rev. B **72**, 094204 (2005).

[47] M.Sekula, S. Pawlus, S. Hensel-Bielowka, J. Ziolo, M. Paluch, M., and C.M. Roland, J. Phys. Chem. B **108**, 4997 (2004).

[48] C.M. Roland, S. Bair, R. Casalini, J. Chem. Phys. **125**, 124508 (2006).

[49] N. Petzold, B. Schmidtke, R. Kahlau, D. Bock, R. Meier, B. Micko, D. Kruk, and E.A. Rössler, J. Chem. Phys. **138**, 12A510 (2013).

[50] A.S. Pensado, A.A.H. Padua,M.J.P. Comunas, and J. Fernandez, J. Phys. Chem. B **112**, 5563 (2008).

[51] O. van den Berg, W.G.F. Sengers, W.F. Jager, S.J. Picken, and M. Wubbenhorst, Macromolecules **37**, 2460 (2004).

[52] R. Casalini, and C.M. Roland, Phys. Rev. Lett. **113**, 085701 (2014).

[53] F. Kremer, A. Schönhals, *Broadband Dielectric Spectroscopy* (Springer, New York, 2003).

[54] A. Abou Elfadl, R. Kahlau, A. Herrmann, V.N. Novikov, E.A. Rössler, Macromolecules, **43**, 3340 (2010).

[55] S. Pawlus, J. Rzoska, J. Ziolo, M. Paluch, and C.M. Roland, Rubber Chem. Technol. **76**, 1106 (2003).

[56] S. Theobald, W. Pechhold, B. Stoll, Polymer **42**, 289 (2001)

[57] R. Casalini, C.M. Roland, S. Capaccioli, J. Chem. Phys. **126**, 184903 (2007).

Table 1. Some parameters of the glass-formers used in the paper.

	T_g, K	T_0, K	γ	Ref. τ_α or η	Ref. γ
sorbitol	268	233±10	0.16	38	39
glycerol	186	177±15	1.8	40,43	39
1-propanol	99	96±5	1.89	41	42
propylene glycol	168	167±8	2.5	43	44
3-fluoroaniline (FAN)	172	187±6	2.7	45	46
dibuthylpthalate	176	156±2	3.2	47	48
propylene carbonate	159	153±8	3.7	43	39
OTP	244	274±2	4	49	39
Cresolphthalein dimethylether (KDE)	314	358±1	4.5	24	39
Phenolphthaleine-dimethyl-ether (PDE)	294	317±2	4.5	23	39
salol	221	250±1	5.2	19	39
polychlorinated biphenyl PCB42	225	257±2	5.5	24	39
BMPC 1,1'-bis(p-methoxy phenyl) cyclohexane	243	287±1	39	27	39
polychlorinated biphenyl PCB62 chlorine content 62%	274	328±1	8.5	24	39
BMMPC 1,1'-di(4-methoxy-5-methyl phenyl) cyclohexane	263	314±2	8.5	24	39
[bmim][NTf2]	181	152±4	2.85	29	50
1,2 polybutadiene (PB)	253	233±8	1.9	44	44
polystyrene (PS)	366	356±38	2.5	51	52
polypropylene glycol (PPG)	202	182±15	2.5	53	39
polyvinylacetate (PVAc)	302	278±4	2.6	28	39
diglycidylether of bisphenol A (DGEBA)	254	260±10	2.8	32	39
1.4 polyisoprene (PI)	202	182±6	3	54	39
poly(methyl phenyl siloxane) (PMPS)	243	261±2	5.6	55	39
PMMA	379	303±54	1.8	56	57
PMMA decamer	288	240±14	2.8	57	57
PMMA tetramer	240	205±4	3.2	57	57
PMMA trimer	210	193±4	3.7	57	57

Figure captions

Fig. 1. (Color online) $\log_{10}\tau_\alpha$ (a) and $d\log_{10}\tau_\alpha/d(T_g/T)$ (b) of salol (symbols). Data for τ_α are from Ref. [19]. Fits of τ_α by VFT (dotted line), Mauro et al [10] (dashed line) and Cole-Grest (solid red line) functions are shown.

Fig. 2. (Color online) a). Second derivative of $\log_{10}\tau_\alpha$ over T_g/T in salol (solid squares). Smooth solid red line is the second derivative of the Cohen-Grest function (Eq.(4)) fit of $\log_{10}\tau_\alpha$. Dashed magenta line is the second derivative of the Mauro et al [10] fitting function, dotted line - the second derivative of the VFT function. The blue solid line is the second derivative of the independent set of data in salol [20]. b). The same (except the data of [20]) with the vertical axis in log-scale. Straight solid lines are the guides for an eye.

Fig. 3 (Color online) a). Second derivative of $\log_{10}\tau_\alpha$ over T_g/T in phenylphthalein dimethyl ether (PDE) (symbols). Data for τ_α are from Ref. [23]. Red solid line is the second derivative of the Cohen-Grest function fit of τ_α. b). The same for polychlorinated biphenyl with chlorine content 62% (PCB62). Data for τ_α are from Ref. [24]. c) and d) are the respective data in the logarithmic scale (symbols) and lines present linear approximations (Eq. (2)).

Fig. 4 (Color online) a). Second derivative of $\log_{10}\tau_\alpha$ over T_g/T in B_2O_3 (solid squares). Solid red line is the second derivative of the Cohen-Grest function (Eq.(4)) fit of $\log_{10}\tau_\alpha$. Dashed blue line is the second derivative of the Mauro et al [10] fitting function, dotted line - the second

derivative of the VFT function. (b) the same plot as (a) but in log scale. The data for τ_α is from Ref. [25]. Straight solid lines are the guides for an eye.

Fig. 5. (Color online) (a) Second derivative of $\log_{10}\tau_\alpha$ over T_g/T in glycerol (symbols). Data for τ_α are from Ref. [26]. Solid red line is the second derivative of the Cohen-Grest function (3) that fits τ_α. (b) The same for propylene carbonate, data for τ_α are from Ref. [23].

Fig. 6 (Color online) a) Second derivative of $\log_{10}\tau_\alpha$ over T_g/T in tri-cresylphosphat (m-TKP) (symbols). Data for τ_α is from Ref. [27]. Solid line presents the second derivative of the Cohen-Grest function that fits τ_α. The same for: b) ethanol (data for τ_α from Ref. [23]; c) polyvinylacetate (PVAc, data for τ_α from Ref. [28]); and d) room-temperature ionic liquid [bmim][NTf2] (data for τ_α from Ref. [29]).

Fig. 7. (Color online) Correlation between γ and $(T_0\text{-}T_g)/T_g$. Non polymeric materials (triangles, in increasing γ order): sorbitol, glycerol, propylene glycol, 3-fluoroaniline (FAN), diglycidylether of bisphenol A (DGEBA), dibuthylpthalate, propylene carbonate, ortho-terphenyl (OTP), cresolphthalein dimethylether (KDE), phenolphthaleine-dimethyl-ether (PDE), salol, cyclohexane polychlorinated biphenyl (PCB42), 1,1'-bis(p-methoxy phenyl) cyclohexane (BMPC), polychlorinated biphenyl (PCB62), 1,1'-di(4-methoxy-5-methyl phenyl) cyclohexane (BMMPC).

Polymers (squares): 1.2 polybutadiene (PB), polystyrene (PS), polypropylene glycol (PPG), polyvinylacetate (PVCa), 1.4 polyisoprene (PI), polymethyl phenyl siloxane (PMPS); polymethyl methacrylate (PMMA) with different molecular weight (circles). The data and references are in the Table 1.

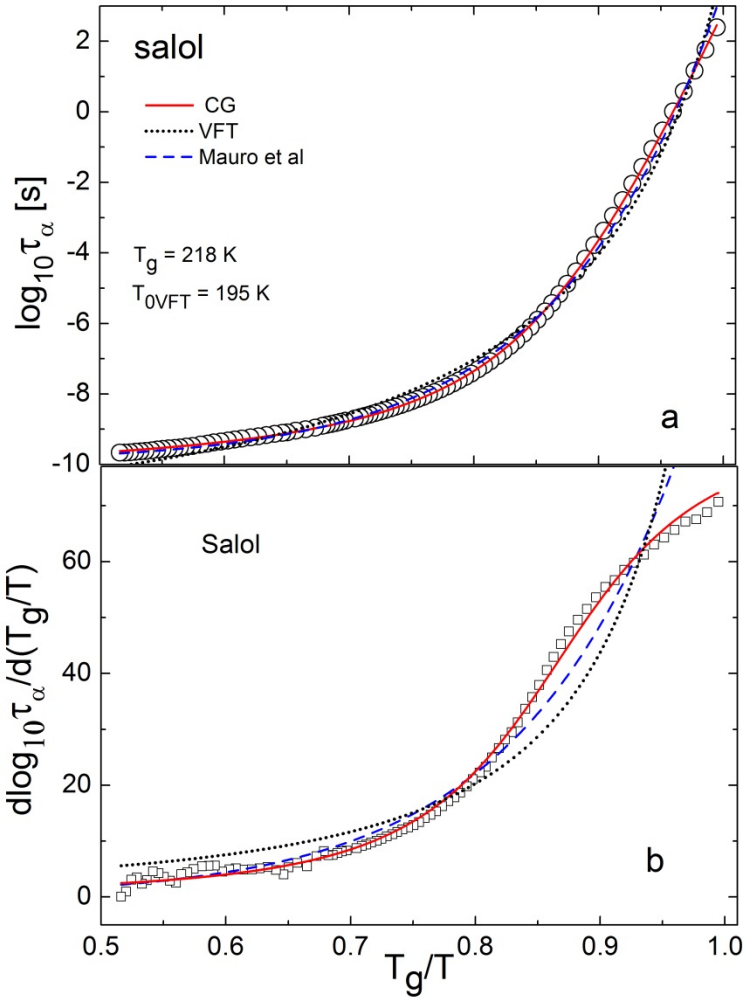
salol
CG
VFT
Mauro et al
T_g = 218 K
T_{0VFT} = 195 K
$\log_{10}\tau_\alpha$ [s]
a
Salol
$d\log_{10}\tau_\alpha/d(T_g/T)$
b
T_g/T

Fig.1

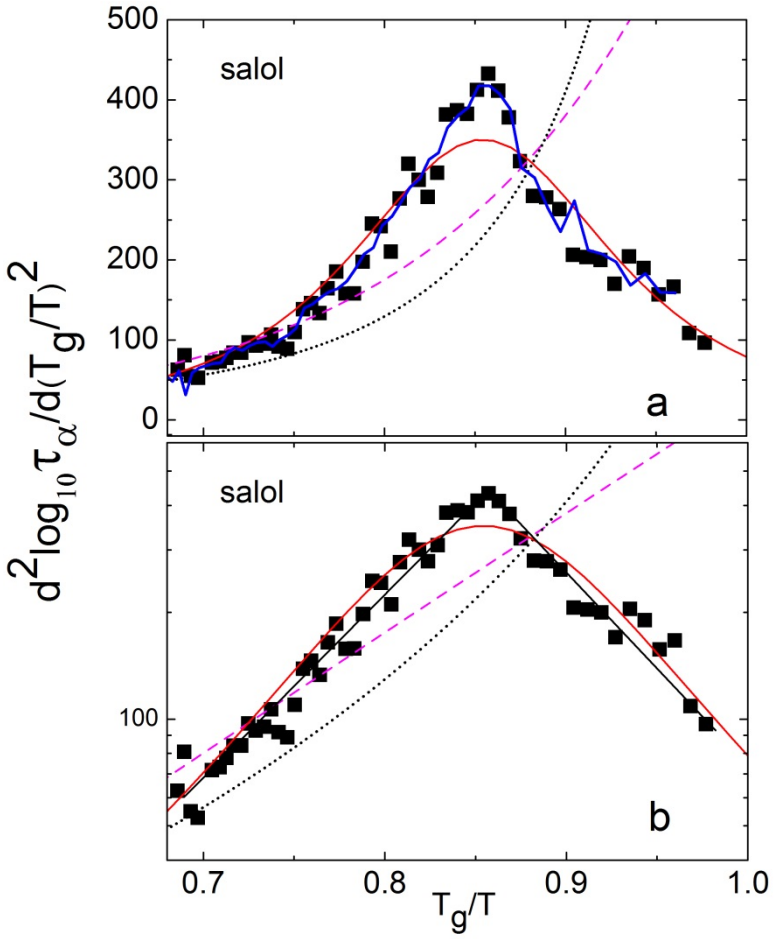
salol
a
salol
b
500
400
300
200
100
0
100
0.7
0.8
0.9
1.0
T_g/T
$d^2\log_{10}\tau_\alpha/d(T_g/T)^2$

Fig. 2

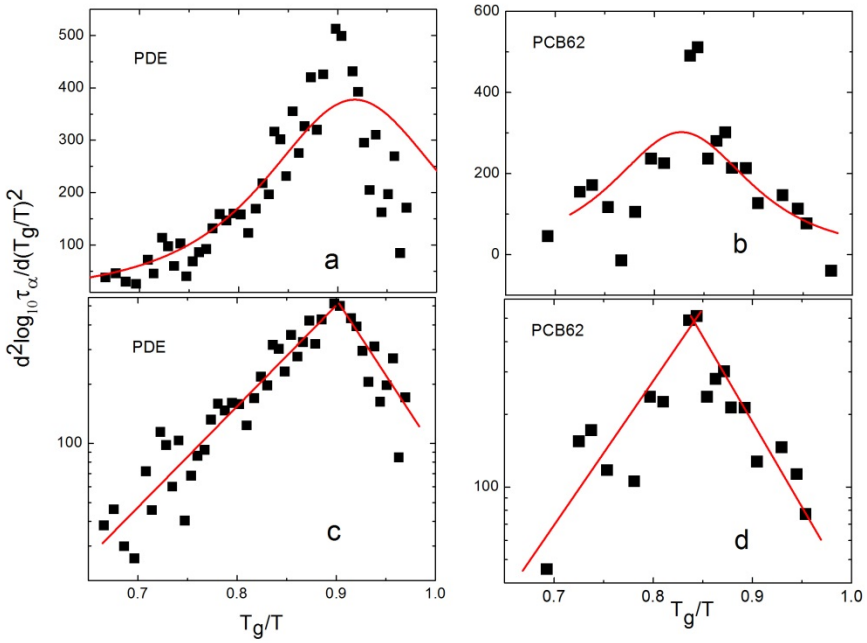

Fig. 3

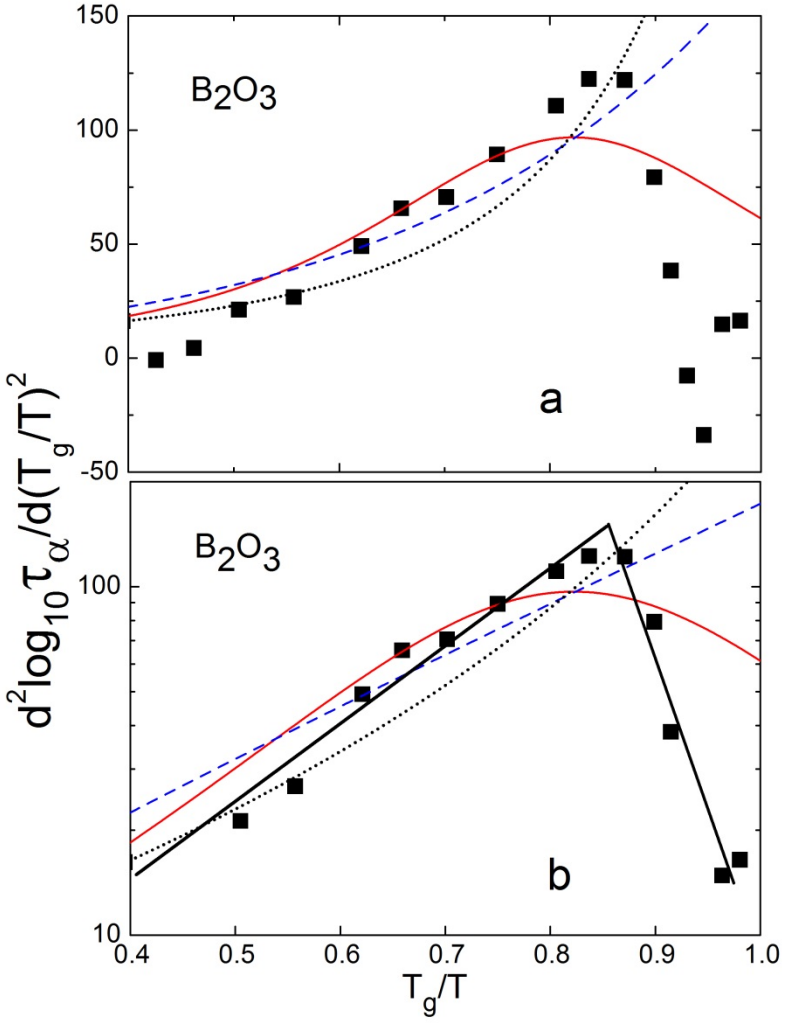
B2O3
a
B2O3
b
150
100
50
0
-50
100
10
0.4
0.5
0.6
0.7
0.8
0.9
1.0
Tg/T
d2log10τα/d(Tg/T)2

Fig. 4

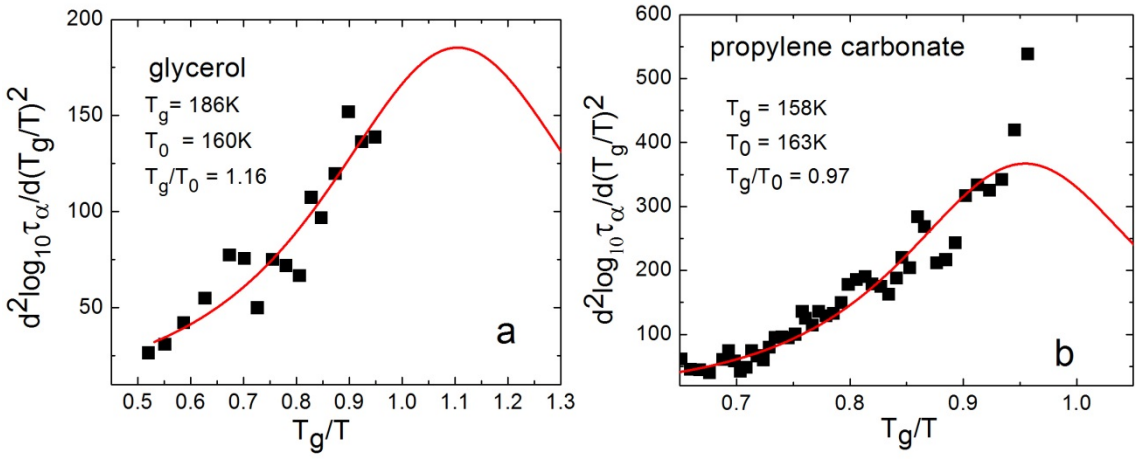
glycerol
T_g= 186K
T_0 = 160K
T_g/T_0 = 1.16
a
$d^2\log_{10}\tau_\alpha/d(T_g/T)^2$
T_g/T
propylene carbonate
T_g = 158K
T_0 = 163K
T_g/T_0 = 0.97
b
$d^2\log_{10}\tau_\alpha/d(T_g/T)^2$
T_g/T

Fig. 5

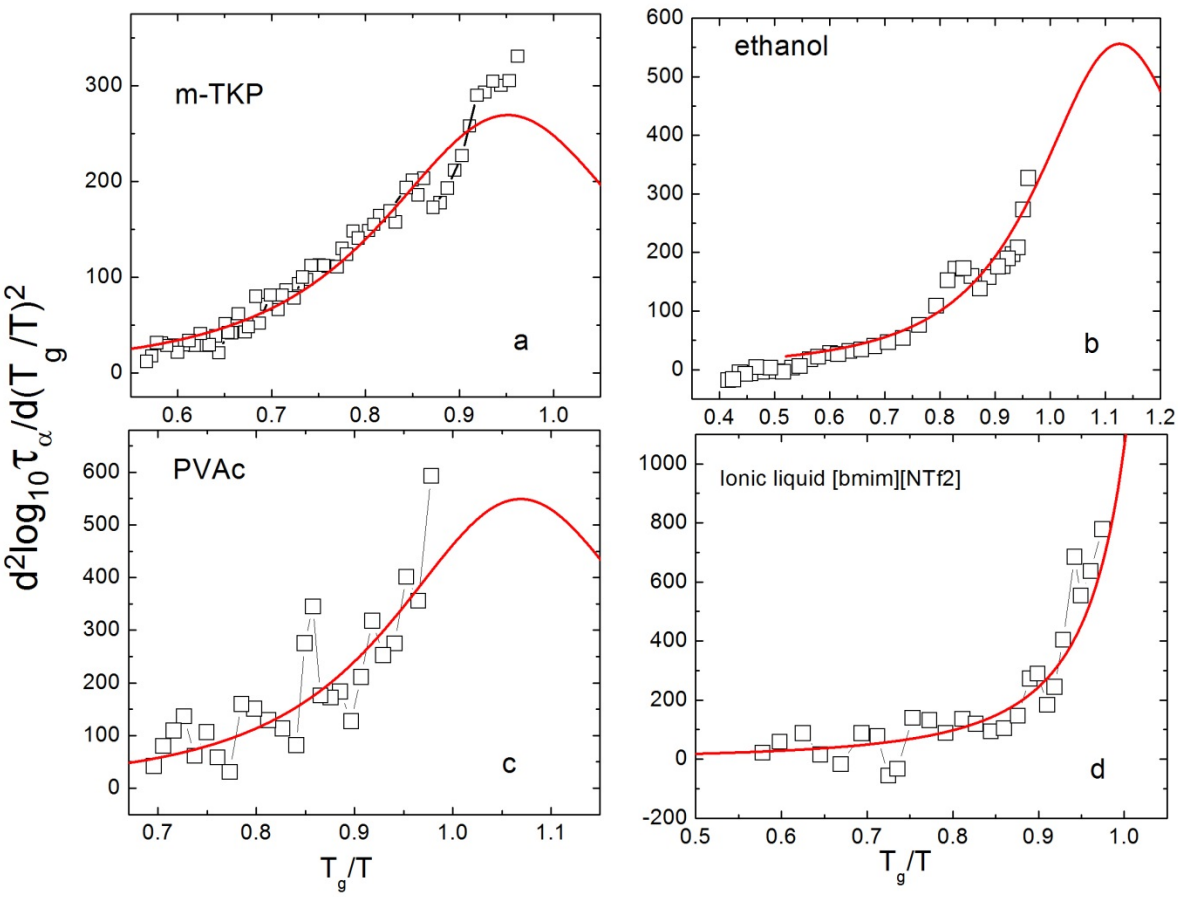
m-TKP
a
ethanol
b
PVAc
c
Ionic liquid [bmim][NTf2]
d
$d^2\log_{10}\tau_\alpha/d(T_g/T)^2$
T_g/T
T_g/T

Fig. 6

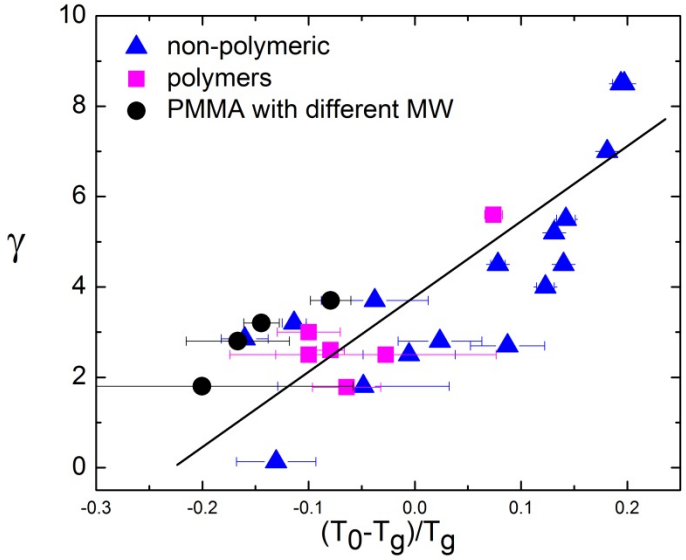
non-polymeric
polymers
PMMA with different MW
γ
(T0-Tg)/Tg
10
8
6
4
2
0
-0.3
-0.2
-0.1
0.0
0.1
0.2

Fig. 7